TECHNICAL TRANSACTIONS | CZASOPISMO TECHNICZNE
ELECTRICAL ENGINEERING | ELEKTROTECHNIKA
1-E/2015

ŽELMÍRA FERKOVÁ*

INFLUENCE OF THE ARRANGEMENT AND SIZES OF MAGNETS ON THE COGGING TORQUE OF PMSM

WPŁYW ROZMIESZCZENIA ORAZ ROZMIARU MEGNESÓW NA MOMENTY ZACZEPOWE W SILNIKACH SYNCHRONICZNYCH Z MAGNESAMI TRWAŁYMI

A b s t r a c t

Two-phase permanent magnet synchronous motors are discussed in this paper and the influence of the magnet sizes on cogging torque (CT) is explored. The cogging torque has been calculated using ANSYS/Maxwell software. In more detail, influences of the magnet size, their positioning and orientation to the CT in two basic rotor types were studied. The cogging torque waveform for critical dimensions has been considered using the FFT analysis. The first rotor type is with semi-arc shaped magnets located on the rotor surface. The second motor type features magnets embedded in its rotor. The shape of the stator magnetic circuit has been predetermined.

Keywords: *cogging torque*, *permanent magnet synchronous motor*, *two-phase motor*

S t r e s z c z e n i e

W artykule omawiane są dwufazowe silniki synchroniczne z magnesami trwałymi oraz analizowany jest wpływ rozmiarów magnesów na momenty zaczepowe. Momenty zaczepowe zostały obliczone za pomocą oprogramowania ANSYS/Maxwell. W szczególności rozpatrywany jest wpływ rozmiaru magnesów, ich ustawienia i orientacji na momenty zaczepowe dla dwóch podstawowych typów wirników. Kształt momentów zaczepowych dla krytycznych rozmiarów został przeanalizowany z użyciem analizy FFT. Pierwszy analizowany typ wirnika zawiera wygięte magnesy zlokalizowane na powierzchni wirnika. Drugi typ silnika zawiera magnesy wbudowane w wirnik. Kształt obwodu magnetycznego stojana został z góry określony.

Słowa kluczowe: *momenty zaczepowe*, *silniki synchroniczne z magnesami trwałymi*, *dwufazowe silniki*

DOI: 10.4467/2353737XCT.15.037.3837

* Ph.D. Eng. Želmíra Ferková, Department of Electrical Engineering, Faculty of Electrical Engineering and Informatics, Technical University of Košice, Slovakia.

1. Introduction

In recent years, the utilisation of permanent magnet synchronous motors has dramatically increased. The advantage of excitation with permanent magnets (PM) is the resulting absence of Joule losses in excitation and especially the elimination of sliding contact. The disadvantage is that excitation is uncontrollable and the recently increasing price of magnets presents an issue as well.

Analysed in the present article is a two-phase two-pole motor with permanent magnets (NdFeB, H_c = –849 000 A/m, B_r = 1.125 T). A ready-made stator stack has been used. The shape and number of stator slots could not be changed.

2. Permanent Magnet Synchronous Motor

In the steady state, behaviour of a two-phase synchronous machine can be described by use of the equations below:

$$\mathbf{U}_1 = R_1\mathbf{I}_1 + \mathrm{j}X_d\mathbf{I}_{1d} + \mathrm{j}X_q\mathbf{I}_{1q} + \mathbf{U}_f \tag{1}$$

$$\mathbf{I}_1 = \mathbf{I}_{1d} + \mathbf{I}_{1q} \tag{2}$$

where:

R_1 – phase resistance,
X_d – d-axis synchronous reactance,
X_q – q-axis synchronous reactance,
$\mathbf{U}_1$ – input voltage,
$\mathbf{I}_1$ – one phase current,
$\mathbf{I}_{1d}$ and $\mathbf{I}_{1q}$ – d and q axis stator currents,
$\mathbf{U}_f$ – voltage (EMF) induced by magnetic excitation flux of the rotor.

Phasor diagrams of over-excited and under-excited motors are presented in Fig. 1. The equations clearly imply induced voltage $\mathbf{U}_f$ of the synchronous machine influences on its behaviour. This depends on the number of turns and the arrangement of the stator winding as well as on the arrangement and size of magnets.

Moreover, the placement of magnets affects the reactance X_d and X_q.

For the PMSM electromagnetic torque, it holds that:

$$T_e = \frac{2}{\omega_{\text{synch}}}\left[\frac{U_1 \cdot U_f}{X_d}\sin\theta + \frac{U_1^2}{2}\left(\frac{1}{X_q} - \frac{1}{X_d}\right)\sin(2\theta)\right] \tag{3}$$

where:

U_1 – the effective values of phase voltage,
U_f – the voltage induced by excitation,
θ – the loading angle [2],
T_e – the electromagnetic torque that neglects CT.

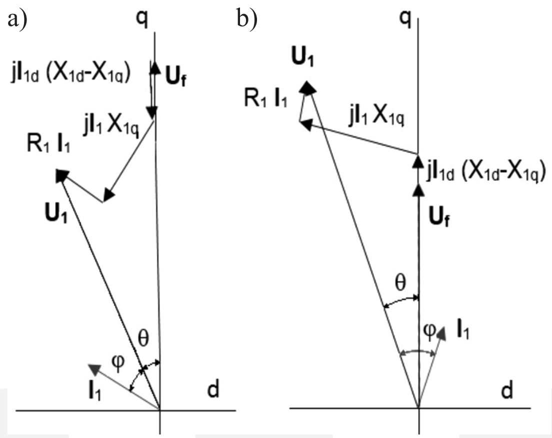

Fig. 1. Phasor diagrams of PMSM, a) over-excited motor, b) under-excited motor

3. Dynamic Model of PMSM

The *d-q* dynamic model is expressed in a rotating frame that moves at a synchronous speed ω_r. The general equation of PMSM working as a motor is as follows:

$$\frac{\mathrm{d}i_d}{\mathrm{d}t} = \frac{u_d}{L_d} - \frac{Ri_d}{L_d} + \frac{L_q}{L_d} p\omega_r i_q \tag{4}$$

$$\frac{\mathrm{d}i_q}{\mathrm{d}t} = \frac{u_q}{L_q} - \frac{Ri_q}{L_q} + \frac{L_d}{L_q} p\omega_r i_d - \Phi \frac{p\omega_r}{L_q} \tag{5}$$

$$T_e = \frac{3}{2} p\left[\Phi i_q + (L_d - L_q) i_d i_q\right] \tag{6}$$

where:
i_d and i_q – the *d* and *q* axis stator currents,
L_d and L_q – the *d* and *q* axis inductances,
u_d and u_q – the *d* and *q* axis stator voltages,
R – phase resistance,
p – the number of pole pairs,
ω_r – the rotor angular speed,
Φ – excitation flux created by the PM.

Electromagnet torque with considered CT is:

$$T_e' = T_e + T_c \tag{7}$$

T_c – depends on stator/rotor angular position.

ANSYS/Maxwell simulation explored the impact of the permanent magnet volumes and arrangement on the cogging torque. Two types of design were chosen, with both motors being two-pole versions.

Type A has rotor surface-mounted magnets. The magnets are semi-arc shaped (rotor surface-mounted magnets). With this type, it can be anticipated that the reactance X_d and X_q are identical.

Type B has two poles made of six magnets embedded in the rotor (Fig. 2). The width, thickness and angles among the magnets of one pole were altered.

a) b)

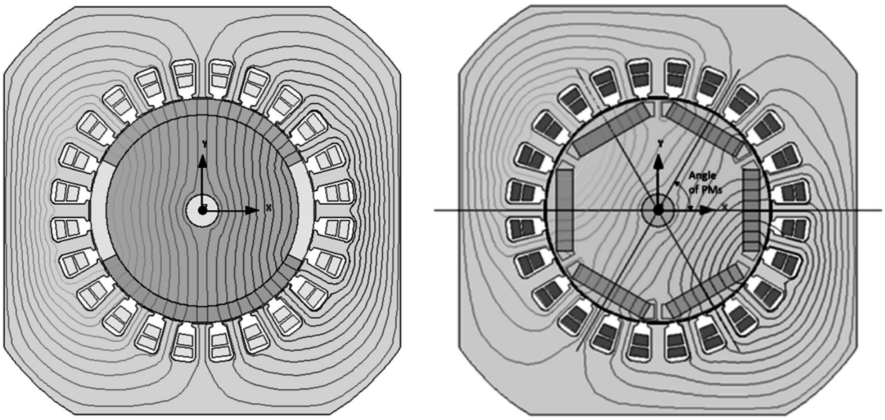

Fig. 2. Design types explored: a) A – motor with rotor surface-mounted magnets, b) B – motor with tangentially embedded magnets.
Dimension of rotor: D_{rot} = 55 mm, rotor length = 26 mm, air gap = 0.5 mm

4. Impact of the Magnet Geometry upon Cogging Torque

When designing 2-pole and 2-phase synchronous motors with permanent magnets, the cogging torque (CT) issue is emerging as more seriously than in the three-phase machines with PM. In this case, the situation becomes worse due to the fact that the magnetic circuit of the stator cannot be changed. The stator has a concentric winding.

The oscillation frequency of the cogging torque depends on the number of slots and is given by the following equation [2]:

$$f_c = \frac{z_1}{p} \cdot f \tag{8}$$

where:
z_1 – the number of stator slots, $z_1 = 24$,
p – the number of pole pairs,
f – the input frequency, $f = 50$ Hz.

Analytical methods for calculating the cogging torque usually neglect the magnetic flux through the stator slot and the saturation of the magnetic circuit. The cogging torque can be computed by the derivative of magnetic energy W produced by permanent magnets with respect to the rotor position angle α:

$$T_c = \frac{\mathrm{d}W}{\mathrm{d}\alpha} \tag{9}$$

Upon adjustment and introduction of coordinate x that represents the air gap length, we have arrived at the equation below:

$$T_c = \frac{D_{2\mathrm{out}}}{2}\frac{\mathrm{d}W}{\mathrm{d}x} \tag{10}$$

where $\alpha = 2x/D_{2\mathrm{uot}}$. It is anticipated that the rotor outer diameter is roughly equal to the stator inner diameter $D_{2\mathrm{out}} \approx D_{1\mathrm{in}}$.

In addition to f_c frequency in the timeline of the CT frequencies that are related to the arrangement of magnets can be found.

The waveform of CT can be, if disregarded is saturation of the magnetic circuitry, described by equation [5]:

$$M_c(\alpha) = \sum_{k=1}^{\infty} M_k \cdot \sin(k \cdot z_1 \alpha + \varphi_k) \tag{11}$$

where:

z_1 – the number of stator slots,
M_k – the related harmonic's amplitude,
φ_k – the phase shift of the respective harmonic,
α – the rotor position.

The cogging torque can by minimised by a proper design [2]. Measures taken in the motor design to minimise the torque ripple include:

- elimination of stator slots,
- skewed slots,
- special shape slots and stator laminations,
- selection of the number of stator slots with respect to the number of poles,
- decentred magnets,
- skewed magnets,
- shifted magnet segments,
- selection of width,
- direction-dependent magnetization of permanent magnets.

ANSYS/Maxwell 2D cogging torque was calculated for the given magnetic circuit of the stator, for two principal rotor types (types A and B; Fig. 2), and for various shapes of magnets.

In type A, which has two arched magnets on the surface of the rotor, the thickness (HM) and also the magnet central angle represented by the *pole embrace* were changed. *Pole embrace* = 1 corresponds to a central angle of 180° and a *pole embrace* = 0.5 corresponds to 90°.

In type B, which is made of 6 magnets forming 2 poles, the magnet thickness (HM), magnet width (SM), and arrangement of magnets that was characterised by the angle between one pole magnets were changed. (Fig. 2b).

In both cases, the magnet length equals the length of the magnetic circuit.

Type A

The dependence of CT from pole embrace is shown in Fig. 3. Multiples of the groove spacing (slot pitch) are represented by the dashed line. The smallest values and the minimum CT are for:

$$\textit{Pole embrace} \approx (\pi - k2\pi/z_1 + \alpha_{od})/\pi \tag{12}$$

where:

$2\pi/z_1$ – slot pitch in degrees ($2\pi/z_1 = 15°$),
k – integer (k = <1.5>),
α_{od} – corresponds to 1/4 of the angle corresponding with the slot opening.

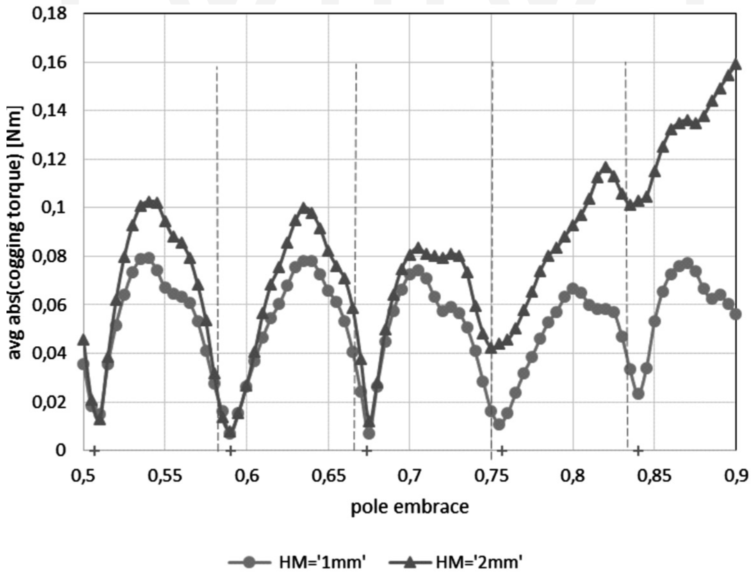

Fig. 3. Average value of absolute values of CT as depending on the pole embrace (HM-thicknesses of magnets)

The smallest CT value can be seen with *pole embrace* = 0.59. This corresponds with the magnet central angle of 106.2°. Different content of higher harmonics in the cogging torque waveform can be for selected *pole embrace* seen in Fig. 4. Prevailing in local max values is the frequency of 1200 Hz (equation (6)).

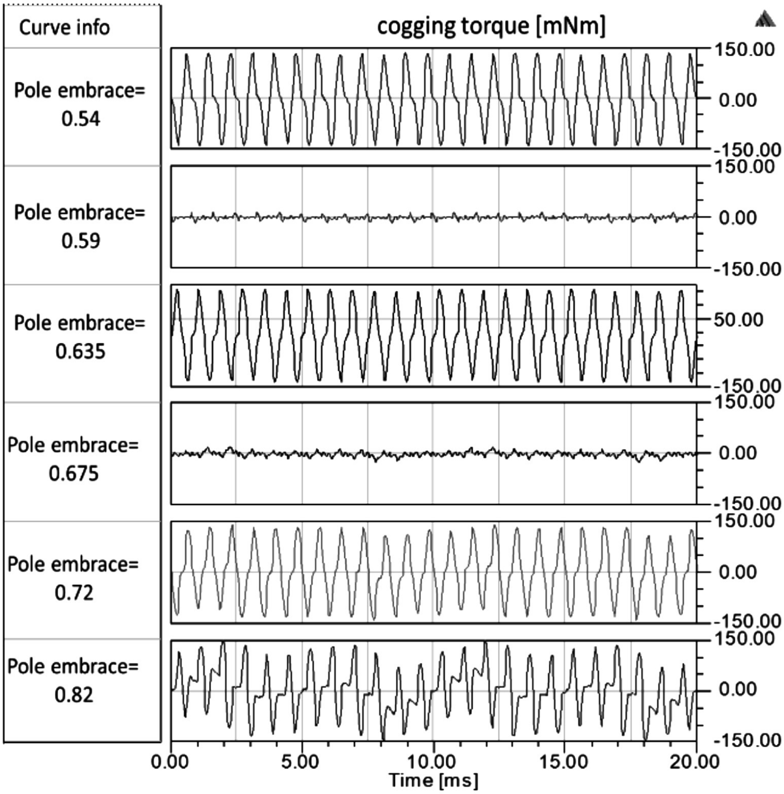

Fig. 4. Cogging torque as a function of time for different *pole embrace*. Rotor speed = 3000 rpm (*pole embrace*: 0.54, 0.59,0.635, 0.675, 0.72, 0.82)

Type B

In this motor type, each pole is composed of three magnets. They were placed in a symmetrical distribution, the angle between the magnets being 60°. Analysis has shown that the arrangement of magnets has significant impact on the cogging torque, and that there exists an angle at which is the cogging torque minimal. CT average value (avgabs[CT]), as depending on the angle between magnets, is shown in Fig. 6. The parameters are the magnet widths (SM) and thicknesses (HM), respectively. The curves show the minimum for the angle of 55°. It is the angle between two magnets of one and the same pole.

The CT waveform dramatically changes with angles to the left and to the right of the minimum. The CT time waveforms for angles of 53°, 55°, and 57° for magnet thicknesses of 3 mm^{-s} and for magnet widths of 18 mm and 19 mm, respectively, are shown in Fig. 7.

The distribution of individual harmonics can be seen in the harmonic analysis shown in Fig. 8. Prevailing are multiples of 1200 Hz. The 1200 Hz frequency is given by the number of slots (equation (8)).

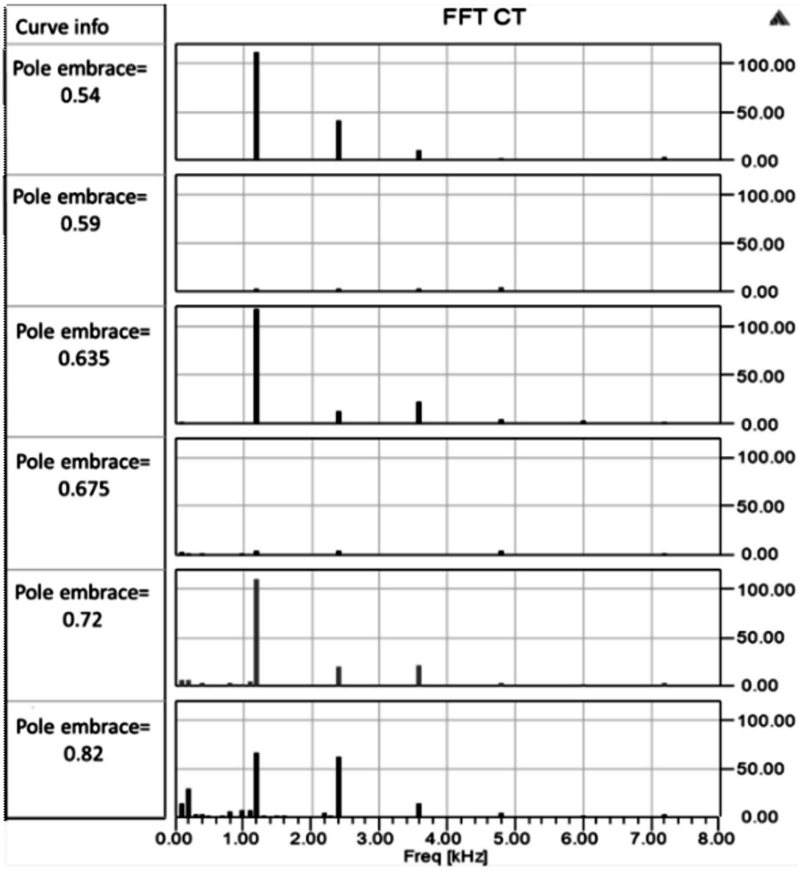

Fig. 5. Harmonic components of the waveform (mag(CT)) given in Fig. 4 (*pole embrace*: 0.54, 0.59, 0.635, 0.675, 0.72, 0.82)

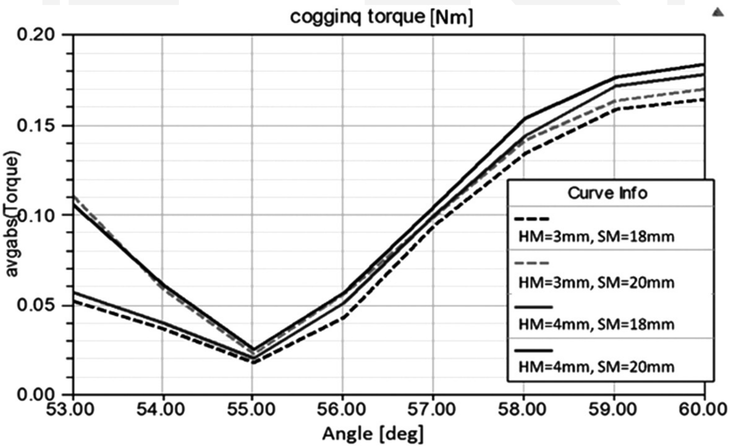

Fig. 6. The average value of the CT (absolute values) depending on the angle between PM (HM – heights of magnets, SM – widths of magnets)

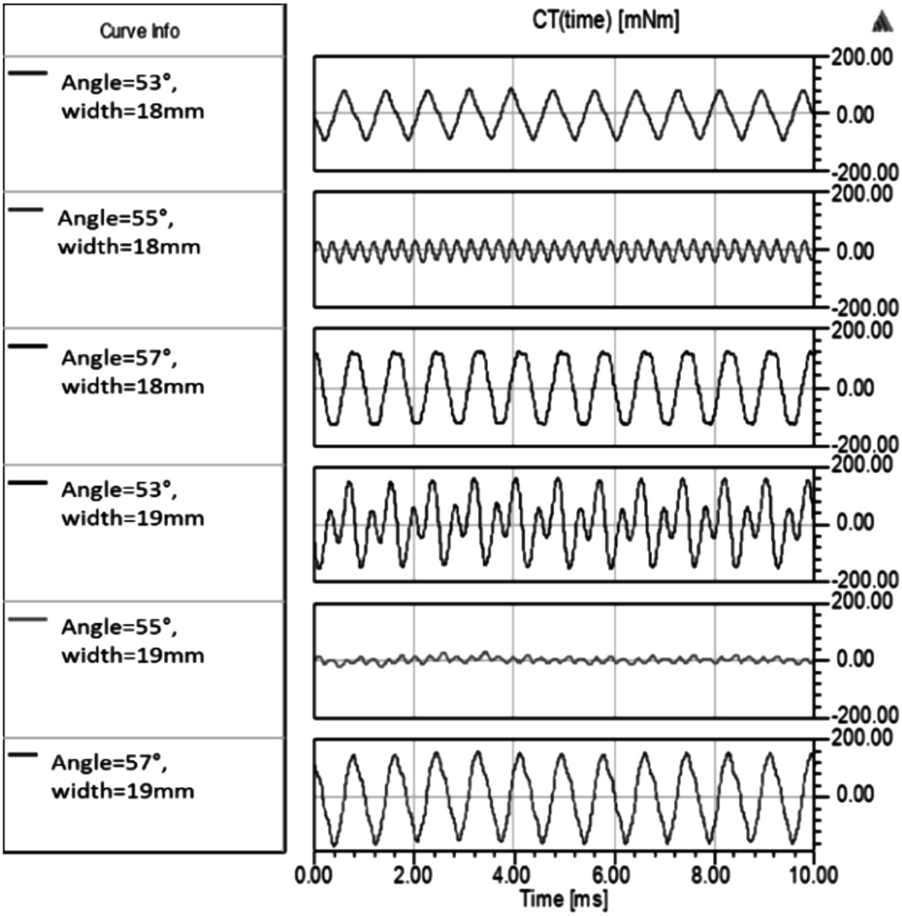

Fig. 7. Cogging torque as function of time for different width of PM and the angle between PM. Rotor speed = 3000 rpm

5. Conclusions

This paper has demonstrated cogging torque dependencies upon the dimensions and geometry of placement of magnets. Fourier analysis of CT waveforms shows a changing spectrum that changes with the arrangement of magnets. Prevailing in both cases are frequencies of f_c = 1200 Hz that are determined by the number of slots, and also multiples of f_c. In areas with a minimum value of CT, these frequencies are significantly suppressed.

Better results, while decreasing cogging torque, can be reached by the skewing of magnets or by the skewing of stator slots. This issue has been resolved although it was not discussed in this article.

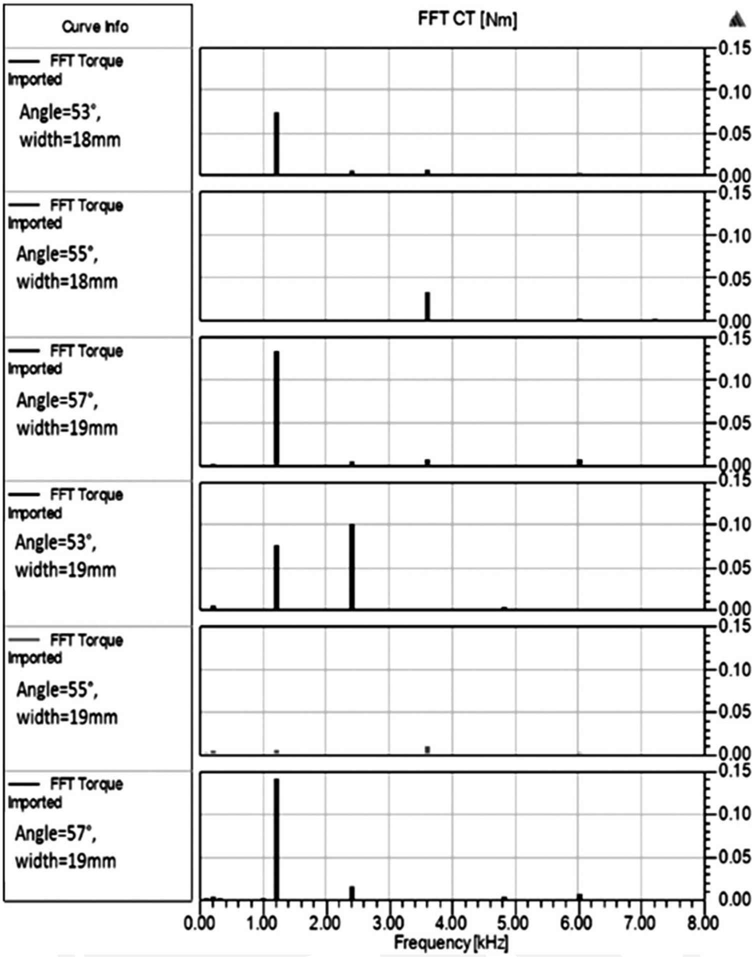

Fig. 8. Harmonic components of the waveform (mag(CT)) given in Fig. 7

Acknowledgement

This work was supported by the Slovak Research and Development Agency under the contract No. SK-CZ-2013-0065 and by the Scientific Agency under the contract No. VEGA 1/0121/15.

References

[1] Pyrhönen L., Jokinenm T., Hrabovcová V., *Design of Rotating Electrical Machines*, John Wiley & Sons, Ltd, 2008.
[2] Gieras J., Wing M., *Permanent Magnet Motor Technology*, Marcel Dekker, USA, 2002.
[3] Gieras J., *Analytical Approach to cogging Torque Calculation of PM Brushless Motors*, IEEE Transactions on Industry Applications, 2004, Vol. 40, No. 5.
[4] Glinka T., *Maszyny elektryczne wzbudzane magnesami trwałymi*, Wydawnictwo Politechniki Śląskiej, Gliwice 2002.
[5] Glinka T., Jakubiec M., *Silniki elektryczne z magnesami trwałymi umieszczonymi na wirniku*, Zeszyty Problemowe – Maszyny Elektryczne, 2005, nr 71, Katowice, p. 103.
[6] Dosiek L., Pillay P., *Cogging Torque Reduction in Permanent Magnet Machines*, IEEE Transactions on Industry Applications, 2007, Vol. 43, No. 65.
[7] Tudorache T., Trifu I., Ghita C., Bostan V., *Improved mathematical model of PMSM taking into account cogging torque oscilations*, Advances in Elektrical and Computer Engineering, 2012, Vol. 12, No. 3, pp. 59–66.
[8] Rosa R., Pistelok P., *The algotithm for the electromagnetic calculations of the concentrated winding permanent magnet synchronous motors*, Zeszyty Problemowe – Maszyny Elektryczne, 2013, nr 4, BORME Komel, Katowice, pp. 161–169.
[9] Mynarek P., Kowol M., *Field-circuit analysis of permanent magnet synchronous motors*, Zeszyty Problemowe – Maszyny Elektryczne, 2014, nr 4, BORME Komel, Katowice, pp. 73–76.
[10] Sekerák P., Hrabovcová V., Pyrhönen J., Kalamen L., Rafajdus P., Onufer M., *Comparison of synchronous motors with different permanent magnet and winding types*, IEEE, Transaction on Magnetics, 2013, Vol. 49, No. 3, ADC, pp. 1256–1263, 9018–9464.
[11] Hruska K., Kindl V., Pechanek R., *Design and FEM analyses of an electrically excited automotive synchronous motor*, 15th International Power Electronics and Motion Control Conference and Exposition 2012, EPE-PEMC 2012 ECCE Europe, art. no. 6397422, pp. LS2e.21–LS2e.27.
[12] Ivančo V., Novotný L., *Mechanika (Mechanics)*, TU Košice, Košice 2010, ISBN 978-80-553-0604-9.
[13] Howe D., Zhu Z.Q., *Cogging torque in permanent magnet machines*, http://www.shef.ac.uk/uni/academic/D-H/eee/md/cogging.html.
[14] Sung S.J., Park S.J., Jang G.H., *Cogging Torque of Brushless DC Motors Due to the Interaction Between the Uneven Magnetization of a Permanent Magnet and Teeth Curvature*, IEEE Transactions on Magnetics, July 2011, Vol. 47, No. 7, pp. 1932–1928.